Kinetic and Spectroscopic Studies on Pentacyano(N-heterocycle)ferrate(II) Rotaxanes of α-Cyclodextrin with Symmetric and Asymmetric Threads

Donal H. Macartney* and Christopher A. Waddling

Department of Chemistry, Queen's University, Kingston, Ontario, Canada K7L 3N6

Received June 9, 1994[⊗]

Metal rotaxane complexes of α-cyclodextrin (α-CD), $[(NC)_5Fe(pyz(CH_2)_nR{\cdot}\alpha\text{-CD})Fe(CN)_5]^{4-}$, have been prepared by the reactions of labile $[Fe(CN)_5OH_2]^{3-}$ ions with pre-threaded dicationic bridging ligands $[pyz(CH_2)_nR]^{2+}$ (pyz = pyrazinium, R = pyrazinium or 4,4′-bipyridinium (bpy), and $n = 8-12$) in aqueous solution. The stability constants for the α-CD inclusion of the ligands, as determined by ^1H NMR spectroscopy, increase with the chain length n and are slightly larger for R = 4,4′-bipyridinium than for pyrazinium head groups. The thermodynamic parameters for the pseudorotaxane equilibria may be correlated in terms of an enthalpy−entropy compensation effect, suggesting that substantial conformation changes and desolvation are involved in the inclusion and dissociation processes. The inclusion of the free ligand by α-CD decreases the rate constants for the formations of the monomeric and dimeric metal complexes from the $[Fe(CN)_5OH_2]^{3-}$ ion. The rate constants for ligand dissociation of $[pyz(CH_2)_nR]^{2+}$ from the metal complexes also decrease upon inclusion of the coordinated bridging ligand. The kinetics of the spontaneous self-assembly of the rotaxane upon mixing the dimer $[(NC)_5Fe(pyz(CH_2)_nR)Fe(CN)_5]^{4-}$ and α-cyclodextrin are consistent with a rate-determining dissociation of a $[Fe(CN)_5]^{3-}$ unit, followed by α-CD inclusion of the semirotaxane and rapid recomplexation by a $[Fe(CN)_5OH_2]^{3-}$ ion to form the rotaxane.

Introduction

Rotaxanes are supramolecular species in which a cyclic molecular bead is threaded by a linear chain bearing bulky end units, which prevent the complex from dissociating into its cyclic and linear molecular components.[1] Stoddart and co-workers have reported elegant procedures for the syntheses of a series of rotaxanes containing tetracationic cyclophanes as the bead, with polyether threads and triisopropyl end groups.[2] Among the other cyclic components which have been employed in the synthesis of rotaxanes, the cyclodextrins, a series of cyclic oligosaccharides normally consisting of six (α-CD), seven (β-CD), or eight (γ-CD) α-(1 → 4)-linked D-(+)-glucopyranose units, have received considerable attention in recent years.[3-15] A number of rotaxanes with symmetric threads, based on α-cyclodextrin, have been reported in which the alkyl chains bear N-heterocyclic,[4-6] carboxylate,[7] or cobalt amine[8,9] end units. An asymmetrical zwitterionic α-CD rotaxane was recently described in which napthalene-2-sulfonate and dimethyl(ferrocenylmethyl)ammonium end groups have been employed.[11] Organic polyrotaxanes have been reported in which 20−40 α-cyclodextrins are strung on poly(iminooligomethylene)[12] or poly(ethylene glycol)biamine[13] chains and subsequently trapped by blocking or capping the chains with nicotinyl or 2,4-dinitrobenzene groups, respectively.

Transition metal rotaxanes have generally been prepared by reacting a semi-rotaxane (bearing one end unit) with a second metal complex or organic end unit.[8,9,11,16,17] We have recently reported the results of kinetic and spectroscopic investigations of the mechanism of the formation of a series of stable α-cyclodextrin rotaxanes of the type $[(NC)_5Fe\{bpy(CH_2)_nbpy{\cdot}\alpha\text{-CD}\}Fe(CN)_5]^{4-}$, where the linear thread is a 1,1″-(α,ω-alkanediyl)bis(4,4′-bipyridinium) dication, $[bpy(CH_2)_nbpy]^{2+}$ ($n = 8-12$), in aqueous solution.[14,15] These species represent the first examples of metal rotaxane complexes that will self-assemble, irrespective of the order of the addition of the α-CD, bridging ligand, and $[Fe(CN)_5]^{3-}$ components.

In this paper we report the results of kinetic and spectroscopic studies on the formation of α-cyclodextrin rotaxanes of the type $[(NC)_5Fe\{pyz(CH_2)_nR{\cdot}\alpha\text{-CD}\}Fe(CN)_5]^{4-}$, where R is pyrazinium or 4,4′-bipyridinium, with $n = 8-12$. The stability constants for the $\{pyz(CH_2)_nR{\cdot}\alpha\text{-CD}\}^{2+}$ inclusion complexes

⊗ Abstract published in *Advance ACS Abstracts,* November 1, 1994.

(1) Schill, G. *Catenanes, Rotaxanes, and Knots*; Academic Press: New York, 1971.
(2) (a) Anelli, P. L.; Spencer, N.; Stoddart, J. F. *J. Am. Chem. Soc.* **1991**, *113*, 5131. (b) Philp, D.; Stoddart, J. F. *Synlett* **1991**, 445. (c) Stoddart, F. *Chem. Br.* **1991**, *27*, 714. (d) Anelli, P. L.; Ashton, P. R.; Ballardini, R.; Balzani, V.; Delgado, M.; Gandolfi, M. T.; Goodnow, T. T.; Kaifer, A. E.; Philp, D.; Pietraszkiewicz, M.; Prodi, L.; Reddington, M. V.; Slawin, A. M. Z.; Spencer, N.; Stoddart, J. F.; Vicent, C.; Williams, D. J. *J. Am. Chem. Soc.* **1992**, *114*, 193.
(3) (a) Stoddart, J. F. *Angew. Chem., Int. Ed. Engl.* **1992**, *31*, 846. (b) Ogino, H. *New J. Chem.* **1993**, *17*, 683.
(4) Yonemura, H.; Saito, H.; Matsushima, S.; Nakamura, H.; Matsuo, T. *Tetrahedron Lett.* **1989**, *30*, 3143.
(5) Saito, H.; Yonemura, H.; Nakamura, H.; Matsuo, T. *Chem. Lett.* **1990**, 535.
(6) Yonemura, H.; Kasahara, M.; Saito, H.; Nakamura, H.; Matsuo, T. *J. Phys. Chem.* **1992**, *96*, 5765.
(7) Watanabe, M.; Makamura, H.; Matsuo, T. *Bull. Chem. Soc. Jpn.* **1992**, *65*, 164.
(8) (a) Ogino, H. *J. Am. Chem. Soc.* **1981**, *103*, 1303. (b) Ogino, H.; Ohata, K. *Inorg. Chem.* **1984**, *23*, 3312.
(9) Yamanari, K.; Shimura, Y. *Bull. Chem. Soc. Jpn.* **1983**, *56*, 2283; **1984**, *57*, 1596.
(10) Rao, T. V. S.; Lawrence, D. S. *J. Am. Chem. Soc.* **1990**, *112*, 3614.
(11) Isnin, R.; Kaifer, A. E. *J. Am. Chem. Soc.* **1991**, *113*, 8188.
(12) (a) Wenz, G. H.; Keller, B. *Angew. Chem., Int. Ed. Engl.* **1992**, *31*, 197. (b) Wenz, G.; van der Bey, E.; Schmidt, L. *Angew. Chem., Int. Ed. Engl.* **1992**, *31*, 783. (c) Wenz, G.; Wolf, F.; Wagner, M.; Kubik, S. *New J. Chem.* **1993**, *17*, 729.
(13) (a) Harada, A.; Li, J.; Kamachi, M. *Nature* **1992**, *356*, 325. (b) Harada, A.; Li, J.; Kamachi, M. *Nature* **1992**, *364*, 516.
(14) Wylie, R. S.; Macartney, D. H. *J. Am. Chem. Soc.* **1992**, *114*, 3136.
(15) Wylie, R. S.; Macartney, D. H. *Supramol. Chem.* **1993**, *3*, 29.
(16) (a) Chambron, J.-C.; Heitz, V.; Sauvage, J.-P. *J. Chem. Soc., Chem. Commun.* **1992**, 1131. (b) Chambron, J.-C.; Harriman, A.; Heitz, V.; Sauvage, J.-P. *J. Am. Chem. Soc.* **1993**, *115*, 6109, 7419. (c) Chambron, J.-C.; Heitz, V.; Sauvage, J.-P. *J. Am. Chem. Soc.* **1993**, *115*, 12378.
(17) Benniston, A. C.; Harriman, A. *Angew. Chem., Int. Ed. Engl.* **1993**, *32*, 1459.

0020-1669/94/1333-5912$04.50/0

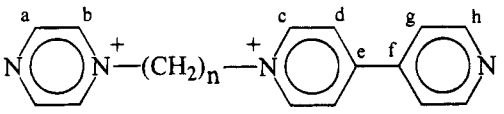

$[pyz(CH_2)_nbpy]^{2+}$ n = 8 - 12

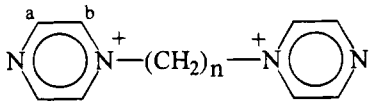

$[pyz(CH_2)_npyz]^{2+}$ n = 8 - 12

have been determined by means of ^{1}H NMR chemical shift titrations and ligand substitution kinetic studies. The kinetics and mechanisms of the formation and ligand dissociation reactions of the semi-rotaxane $[(NC)_5Fe\{pyz(CH_2)_nR\cdot\alpha\text{-CD}\}]^-$ and the self-assembly of the rotaxanes in solution have been studied by using visible and ^{1}H NMR spectroscopy, respectively.

Experimental Section

Materials. The α-cyclodextrin (Aldrich) was dried at 80 °C under reduced pressure for 12 h prior to use. Sodium amminepentacyanoferrate(II) hydrate, $Na_3[Fe(CN)_5NH_3]\cdot 3H_2O$, was prepared by a literature method[18] and recrystallized from concentrated ammonia/methanol solution. The $[Fe(CN)_5OH_2]^{3-}$ ion was generated in solution by the rapid aquation of the ammine salt and kept at low concentrations ($<10^{-4}$ M) to minimize dimerization processes.[19]

The bridging ligands 1,1′-(α,ω-alkanediyl)bis(pyrazinium) diiodide, $[pyz(CH_2)_npyz]I_2$, and (α,ω-alkanediyl)-1-(4,4′-bipyridinium)-1″-(pyrazinium) diodide, $[pyz(CH_2)_nbpy]I_2\cdot xH_2O$, where n = 8−12, were prepared by modifications of the method of Attalla et al.[20]

1,1′-(α,ω-Alkanediyl)bis(pyrazinium) Diiodide. The appropriate α,ω-diiodoalkane was prepared by stirring sodium iodide (50 mmol) with the corresponding α,ω-dibromoalkane (20 mmol, Aldrich) in refluxing acetone for 8 h. The solution was cooled and the sodium bromide precipitate was filtered. Addition of diethyl ether to the filtrate precipitated unreacted sodium iodide and the filtered solution was reduced to dryness. The resultant product was characterized by ^{1}H NMR. The α,ω-diiodoalkane (2 mmol in 15 mL of 1:2 DMF/diethyl ether) was added dropwise with stirring to a solution of pyrazine (40 mmol) in 7 mL of DMF. The reaction mixture was maintained at 50 °C for between one to fifteen days (increasing with increasing chain length). Upon cooling and filtration of any precipitate, 100 mL of diethyl ether was added to the filtrate to precipitate the product from solution. The combined crude product was washed several times with ether to remove residual DMF, and recrystallized from warm ethanol. The yields varied between 60 and 75%. The compounds were characterized by ^{1}H and ^{13}C NMR spectroscopy (presented for n = 12 only; n = 8−11 are very similar) and by elemental analysis (Canadian Microanalytical Services, Delta, B. C.).

$[pyz(CH_2)_8pyz]I_2$. Mp = 166−167 °C. Anal. Calcd for $C_{16}H_{24}N_4I_2$: C, 36.52; H, 4.59; N, 10.69. Found: C, 36.74; H, 4.65; N, 10.40.

$[pyz(CH_2)_9pyz]I_2$. Mp = 79−82 °C. Anal. Calcd for $C_{17}H_{26}N_4I_2$: C, 37.80; H, 4.85; N, 10.37. Found: C, 38.39; H, 4.96; N, 10.29.

$[pyz(CH_2)_{10}pyz]I_2$. Mp = 145−147 °C. Anal. Calcd for $C_{18}H_{28}N_4I_2$: C, 39.01; H, 5.09; N, 10.11. Found: C, 39.05; H, 5.11; N, 9.86.

$[pyz(CH_2)_{11}pyz]I_2$. Mp = 72−74 °C. Anal. Calcd for $C_{19}H_{30}N_4I_2$: C, 40.16; H, 5.32; N, 9.86. Found: C, 40.55; H, 5.35; N, 9.73.

$[pyz(CH_2)_{12}pyz]I_2$. Mp = 93−94 °C. Anal. Calcd for $C_{20}H_{32}N_4I_2$: C, 41.25; H, 5.54; N, 9.62. Found: C, 41.57; H, 5.73; N, 9.14. ^{1}H NMR, δ (D_2O vs TSP): 9.44 (dd, Ha), 9.05 (dd, Hb, $J_{a,b}$ = 4.6 Hz, $J_{a,b'}$ = 1.5 Hz), 4.75 (t, Hα, $J_{\alpha,\beta}$ = 7.5 Hz), 2.07 (m, Hβ), 1.36, 1.34 1.27 (m, Hγ−ζ). ^{13}C NMR, δ (D_2O vs CH_3OH): 151.8 (Ca), 138.5 (Cb), 64.2 (Cα), 31.4 (Cβ), 29.5 (Cζ), 29.4 (Cε), 29.0 (Cδ), 26.2 (Cγ).

(α,ω-Alkanediyl)-1-(4,4′-bipyridinium)-1″-(pyrazinium) Diiodide. The precursor compound $[I(CH_2)_npyz]I$ was prepared by adding the appropriate α,ω-diiodoalkane (1 mmol in 15 mL of 1:1 toluene/DMF) to a solution of pyrazine (2 mmol) in 10 mL of toluene. After refluxing for 20−48 h, the volume was reduced and 100 mL of diethyl ether was added to precipitate the product. The crude product was filtered, washed with water to remove any $[pyz(CH_2)_npyz]I_2$, and dried under reduced pressure. A solution of the $[pyz(CH_2)_nI]I$ (1 mmol in 25 mL of 1:4 DMF/diethyl ether) was added dropwise to a stirred solution of 4,4′-bipyridine (5 mmol) in 5 mL of DMF and maintained at 50 °C for 15 h. The purification and characterizations of the $[pyz(CH_2)_nbpy]I_2\cdot xH_2O$ compounds ($[pyz(CH_2)_{12}bpy]I_2$ was found to be very hygroscopic) were carried out as described for the $[pyz(CH_2)_npyz]I_2$ compounds above.

$[pyz(CH_2)_8bpy]I_2$. Mp = 76−78 °C. Anal. Calcd for $C_{22}H_{28}N_4I_2$: C, 42.60; H, 4.88; N, 9.03. Found: C, 42.65; H, 4.88; N, 8.75.

$[pyz(CH_2)_9bpy]I_2$. Mp = 119−121 °C. Anal. Calcd for $C_{23}H_{30}N_4I_2$: C, 44.82; H, 4.91; N, 9.09. Found: C, 44.86; H, 4.88; N, 9.26.

$[pyz(CH_2)_{10}bpy]I_2\cdot H_2O$. Mp = 135−138 °C. Anal. Calcd for $C_{24}H_{34}N_4I_2O$: C, 44.45; H, 5.29; N, 8.64. Found: C, 44.18; H, 5.04; N, 8.41.

$[pyz(CH_2)_{11}bpy]I_2\cdot 0.5H_2O$. Mp = 50−53 °C. Anal. Calcd for $C_{25}H_{35}N_4I_2O_{0.5}$: C, 45.96; H, 5.40; N, 8.57. Found: C, 45.91; H, 5.54; N, 8.37.

$[pyz(CH_2)_{12}bpy]I_2\cdot 3.5H_2O$. Mp = 78−80 °C. Anal. Calcd for $C_{26}H_{43}N_4O_{3.5}I_2$: C, 43.29; H, 6.01; N, 7.77. Found: C, 42.83; H, 5.21; N, 7.48. ^{1}H NMR: δ (D_2O vs TSP): 9.41 (d, Ha), 9.02 (d, Hb, $J_{a,b}$ = 4.5 Hz), 8.93 (d, Hc), 8.74 (d, Hh), 8.37 (d, Hd, $J_{c,d}$ = 6.8 Hz), 7.89 (d, Hg, $J_{g,h}$ = 6.3 Hz), 4.69 (t, Hα (pyz), $J_{\alpha,\beta}$ = 7.2 Hz), 4.62 (t, Hα′ (bpy), $J_{\alpha',\beta'}$ = 7.4 Hz), 2.02 (m, Hβ), 1.31, 1.27, 1.21 (m, Hγ−ζ). ^{13}C NMR, ζ (D_2O): 153.4 (Ce), 151.0 (Ca), 149.3 (Ch), 145.0 (Cc), 143.8 (Cf), 137.3 (Cb), 126.3 (Cd), 123.1 (Cb), 63.3 (Cα (pyz)), 61.9 (Cα (bpy)), 30.5 (Cβ), 28.6 (Cε−ζ), 28.1 (Cδ), 25.3 (Cγ).

Physical Methods. The ^{1}H and ^{13}C NMR spectra were recorded on Bruker AC-200 and AM-400 instruments in D_2O, employing the residual solvent proton signal (^{1}H) or external CH_3OH (^{13}C) as references. The stability constants for the $[pyz(CH_2)_nR\cdot\alpha\text{-CD}]^{2+}$ species were determined by ^{1}H NMR titrations of the ligand with α-cyclodextrin.[15] For the stability constant determinations, 500 μL solutions of (typically (1−3) × 10^{-3} M) $[pyz(CH_2)_nR]^{2+}$ were titrated with consecutive additions (10−100 μL, using a 250 μL graduated Hamilton gas-tight syringe) of a α-cyclodextrin solution (100 mM) containing the same concentration of the guest species. The solutions were thorougly mixed and allowed to equilibrate for several minutes in the probe (298 K) before the spectrum was acquired.

The kinetic measurements on rapid reactions were performed by using a TDI Model IIA stopped-flow apparatus and data acquisition system (Cantech Scientific). Pseudo-first-order conditions of excess $[pyz(CH_2)_nR]^{2+}$ concentrations ((2.5−40) × 10^{-4} M) over $[Fe(CN)_5OH_2]^{3-}$ concentrations ((2−5) × 10^{-5} M) were employed, and plots of $\ln(A_\infty - A_t)$, monitored at the visible maximum (668 nm) were linear for at least three half-lives. The reported pseudo-first-order rate constants were determined from the average of four replicate experiments. The slower ligand dissociation reactions were followed on Cary 3 and Hewlett-Packard 8452A spectrophotometers at 668 nm for $[Fe(CN)_5(pyz(CH_2)_npyz)]^-$, and 520 and 658 nm for the dissociation of the bpy and pyz ends, respectively, of the $[(NC)_5Fe(bpy\text{-}(CH_2)_npyz)Fe(CN)_5]^{4-}$ complex. The reaction temperature was maintained to within 0.1 °C over the range 10−32 °C by means of external circulating water baths.

Stability Constant Calculations. The cyclodextrin inclusion stability constants K_L^{CD} and K_{ML}^{CD}, for the $[pyz(CH_2)_nR]^{2+}$ and $[(NC)_5Fe(pyz(CH_2)_n)R]^-$ species, respectively, were determined by means of ^{1}H NMR spectroscopy. The concentrations of the included species were determined by integrations of the aliphatic Hβ (and aromatic Hb for R = pyz) proton resonances. Upon inclusion of the ligand, the asymmetry of the α-CD cavity causes these symmetry-related protons to split into two signals, with the upfield signal coincident with that of the free ligand. The concentration of the included ligand is given by eq 1, where A_i and A_T are the area of the downfield peak and the total area,

(18) Brauer, G. *Handbook of Preparative Inorganic Chemistry*, 2nd ed.; Academic Press: New York, 1975; p 1511.
(19) Attalla, M. I.; McAlpine, N. S.; Summers, L. A. *Z. Naturforsch., B.* **1984**, *39B*, 74.
(20) Macartney, D. H. *Rev. Inorg. Chem.* **1988**, *9*, 101 and references therein.

$$[\{L\cdot\alpha\text{-CD}\}] = \frac{2A_i}{A_T}[L]_T \quad (1)$$

respectively. The stability constant K^{CD} is given by eq 2, where $[\alpha\text{-CD}] = [\alpha\text{-CD}]_T - [\{L\cdot\alpha\text{-CD}\}]$ and $[L] = [L]_T - [\{L\cdot\alpha\text{-CD}\}]$.

$$K^{CD} = \frac{[\{L\cdot\alpha\text{-CD}\}]}{[\alpha\text{-CD}][L]} \quad (2)$$

The stability constants were also determined from Simplex optimization and non-linear least-squares fits[21,22] of the ligand substitution kinetic data to the equations for 1:1 host−guest models. The concentration of the included species $[\{L\cdot\alpha\text{-CD}\}]$ was determined from eq 3, where $B = ([L]_T + [\alpha\text{-CD}]_T + (K^{CD})^{-1})$.

$$[\{L\cdot\alpha\text{-CD}\}] = \frac{B - (B^2 - 4[L]_T[\alpha\text{-CD}]_T)^{1/2}}{2} \quad (3)$$

Results

Cyclodextrin−Ligand Inclusion Complexes. The addition of α-cyclodextrin to aqueous solutions of the dicationic ligands $[pyz(CH_2)_nR]^{2+}$ (R = pyrazinium or 4,4′-bipyridinium, n = 8−12) results in the formation of pseudorotaxane inclusion complexes (eq 4) of varying stability. The cyclodextrin

$$[pyz(CH_2)_nR]^{2+} + \alpha\text{-CD} \overset{K_L^{CD}}{\rightleftharpoons} \{pyz(CH_2)_nR\cdot\alpha\text{-CD}\}^{2+} \quad (4)$$

inclusion stability constants (K_L^{CD}) were determined by means of ^{1}H NMR titrations of the ligand with α-CD in D_2O containing 0.10 M NaCl. The inclusion of the ligand in the asymmetric α-CD cavity results in a splitting of the resonances of the symmetry-related protons, as depicted in Figure 1. The observation of pairs of doublets of equal intensity for aromatic protons on both the pyrazinium and bipyridinium rings in the case of the asymmetric ligands $[pyz(CH_2)_nbpy]^{2+}$ indicates that the ligand has no preferred orientation of a particular head group with the narrow or wide rim of the cavity. The inclusion of the ligands also results in upfield shifts in the positions of the H-3 and H-5 protons located on the inside of the α-CD cavity. Similar shifts have been observed previously upon the inclusion of alkyl and aryl substituted pyridines and pyrazines in α- and β-cyclodextrins.[23,24] As the proton resonances of the cyclodextrin exhibit considerable overlap with each other, it is more convenient to determine the inclusion stability constants by monitoring the ligand resonances. The stability constants K_L^{CD} and the corresponding thermodynamic parameters are presented in Table 1. The values of K_L^{CD} measured in this study increase with an increase in the methylene chain length n, as observed previously for $[bpy(CH_2)_nbpy]^{2+}$ (Table 1),[15] and for a given value of n, the trend in K_L^{CD} of $[bpy(CH_2)_nbpy]^{2+} > [pyz(CH_2)_nbpy]^{2+} > [pyz(CH_2)_npyz]^{2+}$ is generally observed. As the temperature is increased the inclusion stability constants decrease. If sufficient α-CD is present to insure complete inclusion at higher temperatures, a study of the effect of temperature on the chemical shift separations may be undertaken. With the $[R(CH_2)_nR]^{2+}$ ligands, where the N-heterocyclic end unit R is pyridinium or 4,4′-bipyridinium, coalescences of the resonances for the symmetry-related ligand protons were observed at temperatures in the range of 50−75 °C.[5,15] Using the $[bpy(CH_2)_npyz]^{2+}$ ligands, a coalescence temperature of approximately 75 °C was determined. With the $[pyz(CH_2)_npyz]^{2+}$ ligands, however, no coalescences were observed up to a temperature of 90 °C, indicating much slower rates of threading the α-CD cavity.

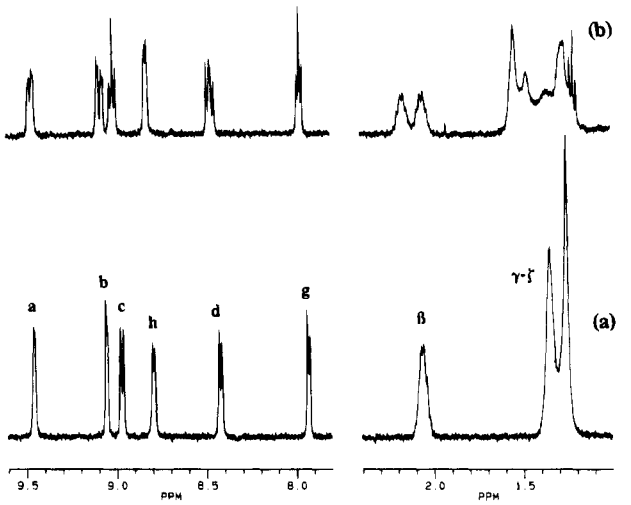

Figure 1. ^{1}H NMR spectra of the (a) $[pyz(CH_2)_{12}bpy]^{2+}$ and (b) $\{pyz(CH_2)_{12}bpy\cdot\alpha\text{-CD}\}^{2+}$ species in D_2O.

Cyclodextrin Rotaxane Complexes. The addition of 1 equiv of the $[Fe(CN)_5OH_2]^{3-}$ ion to a solution containing the cyclodextrin-included N-heterocyclic dicationic ligands results in rapid complexation of one end of the ligand and the formation of a semi-rotaxane species.

$$[Fe(CN)_5OH_2]^{3-} + \{pyz(CH_2)_nR\cdot\alpha\text{-CD}\}^{2+} \rightarrow [Fe(CN)_5\{pyz(CH_2)_nR\cdot\alpha\text{-CD}\}]^- \quad (5)$$

With the asymmetric ligands $[pyz(CH_2)_nbpy]^{2+}$ the semi-rotaxane may consist of either the Fe−pyz or Fe−bpy bonded isomers. The former isomer is the predominant species due to both a greater rate constant for its formation and a smaller rate of ligand dissociation, as discussed below. The addition of one or more further equivalents of the $[Fe(CN)_5OH_2]^{3-}$ ion yields the corresponding rotaxane complex (eq 6). The visible spectra

$$[Fe(CN)_5\{pyz(CH_2)_nR\cdot\alpha\text{-CD}\}]^- + [Fe(CN)_5OH_2]^{3-} \rightarrow [(NC)_5Fe\{pyz(CH_2)_nR\cdot\alpha\text{-CD}\}Fe(CN)_5]^{4-} \quad (6)$$

of the semi-rotaxanes and rotaxanes are dominated by intense metal-to-ligand charge transfer (MLCT) transitions,[19] whose energies depend on the extent of the Fe−L π-back-bonding interactions. For the complexes containing the $[pyz(CH_2)_npyz]^{2+}$ ligands, the λ_{max} values occur at 668 nm ($\epsilon = 1.02 \times 10^4$ M^{-1} cm^{-1}) for the semi-rotaxane and 664 nm ($\epsilon = 1.96 \times 10^4$ M^{-1} cm^{-1}) for the rotaxane with no apparent dependence of the transition energy on the polymethylene chain length n. In the case of the asymmetric rotaxanes, with $L^{2+} = [pyz(CH_2)_nbpy]^{2+}$, two transitions are observed, with the peak at 658 nm ($\epsilon = 1.05 \times 10^4$ M^{-1} cm^{-1}) and shoulder at 520 nm ($\epsilon = 3.5 \times 10^3$ M^{-1} cm^{-1}) corresponding to the coordinated pyz and bpy groups, respectively.

The ^{1}H NMR resonances of the α-CD included ligands experience chemical shifts upon complexation by the $[Fe(CN)_5]^{3-}$ centers similar to those observed for the free ligand upon the formation of the dimer $[(NC)_5Fe(pyz(CH_2)_nR)Fe(CN)_5]^{4-}$. The *ortho* and *meta* protons on the coordinated N-heterocyclic ring shift downfield and upfield, respectively, with similar changes

(21) Cooper, J. W. *Introduction to Pascal for Scientists*; Wiley-Interscience: New York, 1981; pp 185−197.
(22) Forsythe, G. E.; Malcolm, M. A.; Moler, C. B. *Computer Methods for Mathematical Computations*; Prentice-Hall: Englewood Cliffs, NJ, 1977; pp 156−166.
(23) Shortreed, M. E.; Wylie, R. S.; Macartney, D. H. *Inorg. Chem.* **1993**, *32*, 1824.
(24) Wylie, R. S.; Macartney, D. H. *Inorg. Chem.* **1993**, *32*, 1830.

observed in the ^{13}C NMR spectrum. The splitting of the resonances, due to the asymmetry of the α-CD cavity, is maintained in the spectrum of the corresponding rotaxane.

Ligand Substitution Kinetics. The kinetics of the ligand substitution reactions of the aquapentacyanoferrate(II) ion with the free dicationic ligands $[pyz(CH_2)_npyz]^{2+}$ and the α-CD included ligands $\{pyz(CH_2)_npyz{\cdot}\alpha\text{-CD}\}^{2+}$ were measured by using stopped-flow techniques. The reactions were carried out under pseudo-first-order conditions of excess entering ligand concentrations, and linear dependences of k_{obs} on $[L^{2+}]$ were observed for each ligand. In the absence of α-cyclodextrin the second-order rate constants k_f (eq 7) decreased with an increase

$$[Fe(CN)_5OH_2]^{3-} + [pyz(CH_2)_npyz]^{2+} \xrightarrow{k_f} [Fe(CN)_5(pyz(CH_2)_npyz)]^{-} + H_2O \quad (7)$$

in the polymethylene chain length, approaching a limiting value of approximately 6500 M^{-1} s^{-1} (Table 2). Upon inclusion of the ligand by α-CD, the rate constant for the substitution reaction is observed to decrease (Figure 2), reaching a limiting value of k_f^{CD} at high α-CD concentrations (eq 8).

$$[Fe(CN)_5OH_2]^{3-} + \{pyz(CH_2)_npyz{\cdot}\alpha\text{-CD}\}^{2+} \xrightarrow{k_f^{CD}} [Fe(CN)_5\{pyz(CH_2)_npyz{\cdot}\alpha\text{-CD}\}]^{-} \quad (8)$$

The observed second-order rate constants k may be expressed in terms of the specific rate constants k_f and k_f^{CD}, as in eq 9. A

$$k = \frac{k_f[L^{2+}] + k_f^{CD}[\{L{\cdot}\alpha\text{-CD}\}^{2+}]}{[L^{2+}]_T} \quad (9)$$

non-linear least squares fit of the experimental rate constants to eqs 3 and 9 yielded the specific rate constants and the inclusion stability constants presented in Table 2.

With the asymmetric ligands $[pyz(CH_2)_nbpy]^{2+}$, the reaction of the $[Fe(CN)_5OH_2]^{3-}$ ion with an excess of the ligand results in the rapid formation of two coordination isomers. In previous kinetic studies in our laboratory,[25,26] it has been observed that the Fe–pyrazinium bond is more kinetically stable than the Fe–bipyridinium bond, and a spontaneous isomerism (eq 10) would

$$[(NC)_5Fe(bpy(CH_2)_npyz)]^{-} \rightarrow [(NC)_5Fe(pyz(CH_2)_nbpy)]^{-} \quad (10)$$

be expected. The first-order rate constant for the isomerization from $[(NC)_5Fe(bpy(CH_2)_{10}pyz)]^{-}$ to $[(NC)_5Fe(pyz(CH_2)_{10}bpy)]^{-}$ at 25.0 °C was determined from the absorbance changes in the visible maxima of the two isomers, 520 nm (absorbance decrease) and 660 nm (absorbance increase), respectively. The isomerization rate constant, $(1.9 \pm 0.1) \times 10^{-3}$ s^{-1}, is similar to the rate constants measured for the ligand dissociation reaction of $[(NC)_5Fe(bpy(CH_2)_{10}pyz)]^{-}$ in the presence of dimethyl sulfoxide, as described below.

Table 1. Stability Constants (M^{-1}) and Enthalpies (kJ mol^{-1}) and Entropies (J K^{-1} mol^{-1}) of Reaction for the $\{[R(CH_2)_nR'{\cdot}\alpha\text{-CD}\}^{2+}$ Inclusion Complexes in Aqueous Solution (D_2O, 0.10 M NaCl) at 25 °C

n		$pyz(CH_2)_npyz^{2+}$	$pyz(CH_2)_nbpy^{2+}$	$bpy(CH_2)_nbpy^{2+}$ [a]
8	K_L^{CD}	17 ± 2	42 ± 3	72 ± 2
	$\Delta H°$	−27 ± 2	−34 ± 2	−40 ± 3
	$\Delta S°$	−67 ± 6	−80 ± 6	−98 ± 9
9	K_L^{CD}	130 ± 70	220 ± 30	440 ± 30
	$\Delta H°$	−20 ± 1	−25 ± 1	−35 ± 2
	$\Delta S°$	−26 ± 3	−39 ± 3	−68 ± 7
10	K_L^{CD}	1100 ± 100	1400 ± 130	1500 ± 100
	$\Delta H°$	−28 ± 2	−33 ± 3	−35 ± 3
	$\Delta S°$	−37 ± 6	−51 ± 9	−58 ± 9
11	K_L^{CD}	2700 ± 300	2800 ± 330	3400 ± 400
	$\Delta H°$	−38 ± 4	−35 ± 2	−36 ± 3
	$\Delta S°$	−60 ± 12	−52 ± 6	−55 ± 9
12	K_L^{CD}	3200 ± 740	4200 ± 300	3700 ± 500
	$\Delta H°$	−50 ± 3	−60 ± 8	−35 ± 4
	$\Delta S°$	−101 ± 9	−132 ± 24	−50 ± 10

[a] Reference 15.

Table 2. Inclusion Stability Constants for $\{pyz(CH_2)_npyz{\cdot}\alpha\text{-CD}\}^{2+}$ and Rate Constants for the Ligand Substitution Reactions of the $[Fe(CN)_5OH_2]^{3-}$ ion with $[pyz(CH_2)_npyz]^{2+}$ and $\{pyz(CH_2)_npyz{\cdot}\alpha\text{-CD}\}^{2+}$ in Aqueous Solution (I = 0.10 M (NaCl)) at 25.0 °C

ligand	$10^{-3}k_f$, M^{-1} s^{-1}	$10^{-3}k_f^{CD}$, M^{-1} s^{-1}	K_L^{CD}, M^{-1}
$[pyz(CH_2)_8pyz]^{2+}$	11.3 ± 1.3	6.20 ± 0.74	85 ± 30
$[pyz(CH_2)_9pyz]^{2+}$	8.70 ± 0.20	3.20 ± 0.18	170 ± 15
$[pyz(CH_2)_{10}pyz]^{2+}$	6.80 ± 0.30	2.88 ± 0.42	710 ± 230
$[pyz(CH_2)_{11}pyz]^{2+}$	6.60 ± 0.12	3.10 ± 0.17	3600 ± 1400
$[pyz(CH_2)_{12}pyz]^{2+}$	6.50 ± 0.40[a]	3.40 ± 0.13[b]	5400 ± 1900

[a] $\Delta H^{\ddagger}$ = 76 ± 4 kJ mol^{-1}, $\Delta S^{\ddagger}$ = 82 ± 12 kJ mol^{-1}. [b] $\Delta H^{\ddagger}$ = 65 ± 4 kJ mol^{-1}, $\Delta S^{\ddagger}$ = 42 ± 13 kJ mol^{-1}.

The substitution reactions leading to the formations of the iron dimer complexes (eq 11) and the rotaxanes (eq 12) are

$$[Fe(CN)_5OH_2]^{3-} + [(NC)_5Fe(pyz(CH_2)_npyz)]^{-} \xrightarrow{k_{f2}} [(NC)_5Fe(pyz(CH_2)_nR)Fe(CN)_5]^{4-} \quad (11)$$

$$[Fe(CN)_5OH_2]^{3-} + [(NC)_5Fe\{pyz(CH_2)_nR{\cdot}\alpha\text{-CD}\}]^{-} \xrightarrow{k_{f2}^{CD}} [(NC)_5Fe\{pyz(CH_2)_nR{\cdot}\alpha\text{-CD}\}Fe(CN)_5]^{4-} \quad (12)$$

slower, as a result of a decrease in the formal charge on the entering "ligands" $[Fe(CN)_5(pyz(CH_2)_nR)]^{-}$ and $[Fe(CN)_5\{pyz(CH_2)_nR{\cdot}\alpha\text{-CD}\}]^{-}$, respectively, compared with the dicationic ligands. At 25.0 °C and I = 0.10 M (NaCl) the values of k_{f2} and k_{f2}^{CD} are $(2.0 \pm 0.2) \times 10^3$ M^{-1} s^{-1} and $(1.58 \pm 0.10) \times 10^3$ M^{-1} s^{-1}, respectively, for n = 10.

The effects of α-cyclodextrin inclusion of the coordinated ligand, $[R(CH_2)_npyz]^{2+}$, on the kinetics of its dissociation from the $[Fe(CN)_5(R(CH_2)_npyz)]^{-}$ ion have been investigated. The reaction is facilitated by the addition of dimethyl sulfoxide (0.2 M DMSO) to trap the $[Fe(CN)_5]^{3-}$ intermediate and form an inert $[Fe(CN)_5DMSO]^{3-}$ product (eq 13). The addition of α-CD

$$[Fe(CN)_5(pyz(CH_2)_npyz)]^{-} + DMSO \xrightarrow{k_d} [Fe(CN)_5DMSO]^{3-} + [pyz(CH_2)_npyz]^{2+} \quad (13)$$

(25) Macartney, D. H.; Warrack, L. J. *Can. J. Chem.* **1989**, *67*, 1774.
(26) Foucher, D. A.; Macartney, D. H.; Warrack, L. J.; Wilson, J. P., *Inorg. Chem.* **1993**, *32*, 3425.

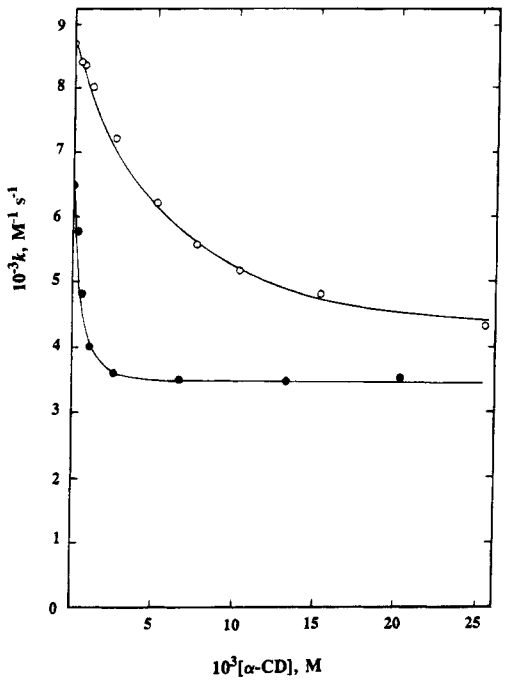

Figure 2. Plots of k against [α-CD] for the reactions of the $[Fe(CN)_5OH_2]^{3-}$ ion with the (○) $[pyz(CH_2)_9pyz]^{2+}$ and (●) $[pyz(CH_2)_{12}pyz]^{2+}$ ligands at 25.0 °C (I = 0.10 M (NaCl)).

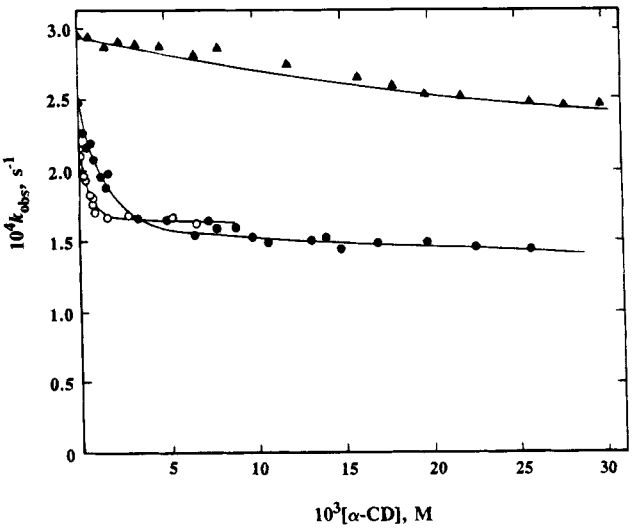

Figure 3. Plots of k_{obs} against [α-CD] for the ligand dissociation reactions of the (▲) $[(NC)_5Fe(pyz(CH_2)_8pyz)Fe(CN)_5]^{4-}$, (●) $[(NC)_5Fe(pyz(CH_2)_{10}pyz)Fe(CN)_5]^{4-}$, and (○) $[(NC)_5Fe(pyz(CH_2)_{12}pyz)Fe(CN)_5]^{4-}$ ions in the presence of 0.20 M DMSO (I = 0.10 M (NaCl)) at 25.0 °C.

to the reaction solution results in a decrease in the ligand dissociation rate constant (Figure 3) upon the α-CD inclusion of the coordinated ligand (eqs 14 and 15). The observed first-

$$[Fe(CN)_5(pyz(CH_2)_npyz)]^- + \alpha\text{-CD} \overset{K_{ML}^{CD}}{\rightleftharpoons} [Fe(CN)_5\{pyz(CH_2)_npyz\cdot\alpha\text{-CD}\}]^- \quad (14)$$

$$[Fe(CN)_5\{pyz(CH_2)_npyz\cdot\alpha\text{-CD}\}]^- + DMSO \xrightarrow{k_d^{CD}} [Fe(CN)_5DMSO]^- + \{pyz(CH_2)_npyz\cdot\alpha\text{-CD}\}^{2+} \quad (15)$$

order dissociation rate constant may be expressed in terms of the specific rate constants k_d and k_d^{CD} and the α-CD inclusion stability constant for $[Fe(CN)_5\{R(CH_2)_npyz\cdot\alpha\text{-CD}\}]^-$ in the reaction medium (eq 16). The ligand dissociation reactions were

$$k_{obs} = \frac{k_d + k_d^{CD}K_{ML}^{CD}[\alpha\text{-CD}]}{1 + K_{ML}^{CD}[\alpha\text{-CD}]} \quad (16)$$

carried out in the presence of an excess of the free ligand L^{2+} (to ensure formation of the monomeric iron complex), which will also compete for inclusion in the α-CD cavity. This competing inclusion process was accounted for in calculating the available [α-CD], using the data in Table 1. The values of k_d^{CD} and K_{ML}^{CD}, determined by means of a least-squares fit of the kinetic data to eq 16, are presented along with the rate and activation parameters for the free ligand reactions in Table 3.

The rate constants for the dissociation of the iron dimer and rotaxane complexes were also measured using DMSO as the entering ligand. For the symmetric $[pyz(CH_2)_npyz]^{2+}$ bridging ligands a monophasic first-order dissociation was observed, indicating that the rate constants for both steps in the process are very similar. For the asymmetric $[pyz(CH_2)_nbpy]^{2+}$ ligands a biphasic decay was observed, with the faster step associated with the more labile bipyridinium end of the complex (eq 17),

$$[(NC)_5Fe(pyz(CH_2)_nbpy)Fe(CN)_5]^{4-} + DMSO \xrightarrow{k_{db}} [(NC)_5Fe(pyz(CH_2)_nbpy)]^- + [Fe(CN)_5DMSO]^{3-} \quad (17)$$

followed by the slower dissociation of the iron–pyrazinium bond (eq 18). The rate constants for the two steps differ by

$$[(NC)_5Fe(pyz(CH_2)_nbpy)]^- + DMSO \xrightarrow{k_{dp}} [Fe(CN)_5DMSO]^{3-} + [pyz(CH_2)_nbpy]^{2+} \quad (18)$$

approximately an order of magnitude and it was possible to analyze the biphasic curve as two first-order processes. In the presence of α-CD both reactions are slowed owing to the inclusions of the bridging and monodentate ligands in the rotaxane (eq 19) and semi-rotaxane (eq 20) species, respectively.

$$[(NC)_5Fe\{pyz(CH_2)_nbpy\cdot\alpha\text{-CD}\}Fe(CN)_5]^{4-} + DMSO \xrightarrow{k_{db}^{CD}} [(NC)_5Fe\{pyz(CH_2)_nbpy\cdot\alpha\text{-CD}\}]^- + [Fe(CN)_5DMSO]^{3-} \quad (19)$$

$$[(NC)_5Fe\{pyz(CH_2)_nbpy\cdot\alpha\text{-CD})]^- + DMSO \xrightarrow{k_{dp}^{CD}} [Fe(CN)_5DMSO]^{3-} + \{pyz(CH_2)_nbpy\cdot\alpha\text{-CD}\}^{2+} \quad (20)$$

The rate constants k_{db}, k_{dp}, k_{db}^{CD}, and k_{dp}^{CD} were determined at 25.0 °C using eq 16 and are presented in Table 4, along with the corresponding activation parameters.

Rotaxane Self-Assembly. The rotaxane may also be formed by the reaction of the iron dimer complex $[(NC)_5Fe(pyz(CH_2)_nR)Fe(CN)_5]^{4-}$ with an excess of α-cyclodextrin, and the kinetics of this process monitored by ^1H NMR spectroscopy (Figure 4). The symmetry-related proton resonances of the bridging ligand of the dimer (Figure 4(a)) are separated into pairs of peaks as the rotaxane is formed (Figure 4(e)). The direct inclusion of the dimer by threading through the α-CD cavity (5.5 Å diameter) is prevented by the bulky $[Fe(CN)_5]^{3-}$ units (9.0 Å diameter). The rotaxane formation occurs by a mechanism involving the relatively slow dissociation of a $[Fe(CN)_5]^{3-}$ unit, followed by the formation of a semirotaxane, $[(NC)_5Fe\{pyz(CH_2)_nR\cdot\alpha\text{-CD}\}]^-$ and the subsequent rapid re-complexation by a $[Fe(CN)_5OH_2]^{3-}$ ion to produce the rotaxane.

Table 3. Cyclodextrin Inclusion Stability Constants and Ligand Dissociation Rate and Activation Parameters for the Reactions of $[(NC)_5Fe(pyz(CH_2)_npyz)]^-$ and $[(NC)_5Fe\{PYZ(ch_2)_npyz\cdot\alpha\text{-CD}\}]^-$ Species with Dimethyl Sulfoxide[a]

n	10^4k_d, s^{-1}	$\Delta H^{\ddagger}$, kJ mol^{-1}	$\Delta S^{\ddagger}$, J K^{-1} mol^{-1}	$10^4k_d^{CD}$, s^{-1}	$\Delta H^{\ddagger}$, kJ mol^{-1}	$\Delta S^{\ddagger}$, J K^{-1} mol^{-1}	K_{ML}^{CD}, M^{-1}
8	2.94	110 ± 1	57 ± 3	1.3 ± 0.3	101 ± 1	26 ± 3	15 ± 4
9	2.58	110 ± 1	55 ± 3	1.3 ± 0.1	112 ± 5	57 ± 14	96 ± 16
10	2.48	101 ± 2	25 ± 6	1.40 ± 0.02	103 ± 2	27 ± 6	770 ± 90
11	2.29	113 ± 1	64 ± 3	1.48 ± 0.02	119 ± 2	60 ± 6	1530 ± 170
12	2.16	102 ± 1	28 ± 3	1.65 ± 0.03	102 ± 1	26 ± 3	5700 ± 1300

[a] At 25.0 °C, I = 0.10 M (NaCl).

Table 4. Ligand Dissociation Rate and Activation Parameters for the Reactions of $[(NC)_5Fe(bpy(CH_2)_npyz)Fe(CN)_5]^{4-}$ and $[(NC)_5Fe\{bpy(CH_2)_npyz\cdot\alpha\text{-CD}\}Fe(CN)_5]^{4-}$ Species with Dimethyl Sulfoxide at 25.0 °C

n	k_d, s^{-1}	$\Delta H^{\ddagger}$ kJ mol^{-1}	$\Delta S^{\ddagger}$, J K^{-1} mol^{-1}	k_d^{CD}, s^{-1}	$\Delta H^{\ddagger}$ kJ mol^{-1}	$\Delta S^{\ddagger}$ J K^{-1} mol^{-1}
			Fe−bpy			
8	1.59×10^{-3}	112 ± 3	77 ± 8	1.05×10^{-3}	118 ± 2	95 ± 7
9	1.49×10^{-3}	98 ± 1	30 ± 2	1.08×10^{-3}	108 ± 2	60 ± 6
10	1.47×10^{-3}	117 ± 2	93 ± 6	1.11×10^{-3}	121 ± 2	104 ± 7
11	1.52×10^{-3}	101 ± 2	43 ± 7	1.18×10^{-3}	109 ± 1	64 ± 2
12	1.39×10^{-3}	112 × 3	79 ± 9	1.21×10^{-3}	119 ± 3	99 ± 9
			Fe−pyz			
8	2.80×10^{-4}	101 ± 1	27 ± 3	1.82×10^{-4}	119 ± 2	82 ± 7
9	3.05×10^{-4}	109 ± 1	53 ± 3	1.53×10^{-4}	125 ± 12	101 ± 35
10	2.36×10^{-4}	105 ± 3	39 ± 8	1.85×10^{-4}	111 ± 4	58 ± 12
11	2.40×10^{-4}	101 ± 5	23 ± 13	1.61×10^{-4}	114 ± 4	66 ± 11
12	2.83×10^{-4}	103 ± 6	34 ± 18	1.91×10^{-4}	112 ± 7	61 ± 20

The extent of the rotaxane formation is determined by the stability constant of the semirotaxane species and the kinetics of approach to equilibrium is given by eq 21, where $[L]_0$ is the

$$\ln\left|\frac{[L]_0 - [L\cdot CD]_e}{[L\cdot CD]_t - [L\cdot CD]_e}\right| = kt \qquad (21)$$

initial dimer concentration, and $[L\cdot CD]_t$ and $[L\cdot CD]_e$ are the concentrations of the rotaxane (from eq 1) at time t and at equilibrium, respectively. The equilibrium concentrations of the rotaxanes were found to be in good agreement with the values that would be determined from eq 2 using the stability contants for the pseudo-rotaxane species, $\{pyz(CH_2)_nR\cdot\alpha\text{-CD}\}^{2+}$ (Table 1). The first-order rate constants determined for the self-assembly processes at 25 °C are presented in Table 5.

Discussion

The stability constants K_L^{CD} for the formation of the cyclodextrin inclusion complexes of the N-heterocyclic dicationic ligands exhibit dependences on the length of the polymethylene chain between the N-heterocyclic end groups and to a smaller extent to the nature of the N-heterocycle. The increase in the stability constants with an increase in the chain length n has been observed previously for several α-CD inclusion systems, in which the end groups have been 4,4′-bipyridinium,[15] pyridinium,[4] or $-CO_2-$.[7] As the chain length is decreased the charged end groups are drawn further towards the more hydrophobic cyclodextrin interior, destabilizing the pseudorotaxane. Similar stability constants are observed for the semirotaxanes (K_{ML}^{CD}), again indicating that the hydrophobic polymethylene chain length is more important than the nature of the end unit in determining the strength of the binding.

With the binding constants for the ligands in this study and the values previously determined for the $[bpy(CH_2)_nbpy]^{2+}$ ligand series, a trend in K_L^{CD} for a given polymethylene chain length n of $[bpy(CH_2)_nbpy]^{2+}$ > $[bpy(CH_2)_npyz]^{2+}$ > $[pyz(CH_2)_npyz]^{2+}$ emerges. An explanation of this trend requires a consideration of the kinetics of the threading and dethreading processes. The first step in the formation of the pseudorotaxanes with the dicationic ligands would be the inclusion of a N-heterocyclic cation in the α-CD cavity, before threading

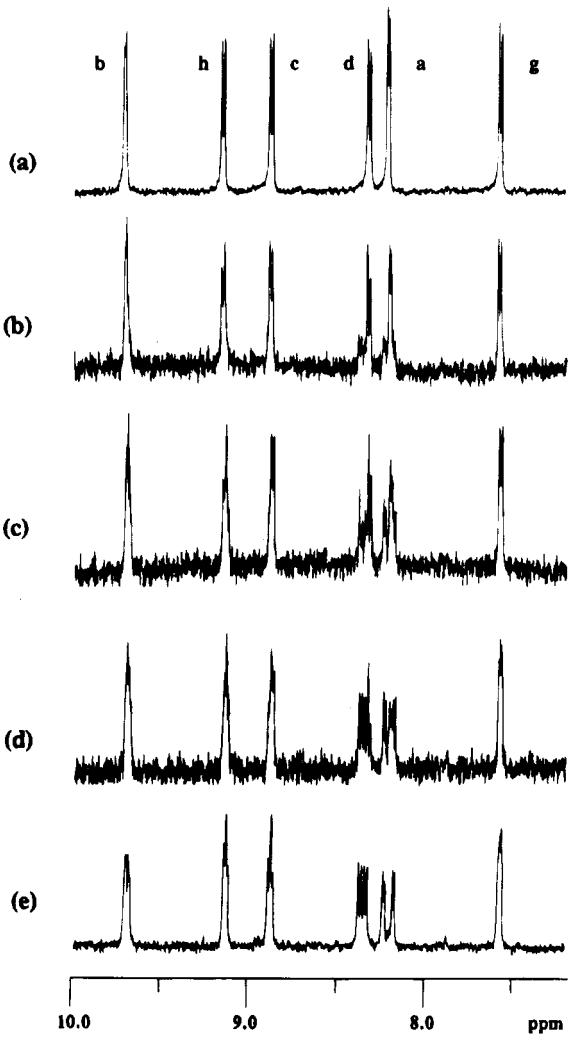

Figure 4. ^1H NMR spectra of the aromatic protons as a function of time for the self-assembly of the $[(NC)_5Fe\{pyz(CH_2)_9bpy\cdot\alpha\text{-CD}\}Fe(CN)_5]^{4-}$ rotaxane upon the addition of α-CD (4.5×10^{-2} M) to the $[(NC)_5Fe\{pyz(CH_2)_9bpy\}Fe(CN)_5]^{4-}$ dimer (3×10^{-3} M) in D_2O (0.10 M NaCl) at 25.0 °C. Spectra were recorded at (a) 0 min, (b) 5 min, (c) 9 min, (d) 20 min, and (e) 65 min.

Table 5. Kinetic Parameters for the Self-Assembly of the Cyclodextrin Rotaxane Complexes $[(NC)_5Fe\{R(CH_2)_npyz\cdot\alpha\text{-}CD\}Fe(CN)_5]^{4-}$ in Aqueous Solution at 25 °C (0.10 M NaCl)[a]

rotaxane	k, s^{-1}
$[(NC)_5Fe\{pyz(CH_2)_8pyz\cdot\alpha\text{-}CD\}Fe(CN)_5]^{4-}$	$(1.7 \pm 0.2) \times 10^{-4}$ [b]
$[(NC)_5Fe\{pyz(CH_2)_9pyz\cdot\alpha\text{-}CD\}Fe(CN)_5]^{4-}$	$(2.5 \pm 0.3) \times 10^{-4}$ [c]
$[(NC)_5Fe\{pyz(CH_2)_{10}pyz\cdot\alpha\text{-}CD\}Fe(CN)_5]^{4-}$	$(2.6 \pm 0.1) \times 10^{-4}$ [c]
$[(NC)_5Fe\{pyz(CH_2)_{11}pyz\cdot\alpha\text{-}CD\}Fe(CN)_5]^{4-}$	$(3.2 \pm 0.1) \times 10^{-4}$ [c]
$[(NC)_5Fe\{pyz(CH_2)_{12}pyz\cdot\alpha\text{-}CD\}Fe(CN)_5]^{4-}$	$(2.0 \pm 0.1) \times 10^{-4}$ [c]
$[(NC)_5Fe\{bpy(CH_2)_8pyz\cdot\alpha\text{-}CD\}Fe(CN)_5]^{4-}$	$(1.0 \pm 0.1) \times 10^{-3}$ [d]
$[(NC)_5Fe\{bpy(CH_2)_9pyz\cdot\alpha\text{-}CD\}Fe(CN)_5]^{4-}$	$(1.1 \pm 0.1) \times 10^{-3}$ [e]
$[(NC)_5Fe\{bpy(CH_2)_{10}pyz\cdot\alpha\text{-}CD\}Fe(CN)_5]^{4-}$	$(1.0 \pm 0.1) \times 10^{-3}$ [e]
$[(NC)_5Fe\{bpy(CH_2)_{11}pyz\cdot\alpha\text{-}CD\}Fe(CN)_5]^{4-}$	$(1.1 \pm 0.1) \times 10^{-3}$ [e]
$[(NC)_5Fe\{bpy(CH_2)_{12}pyz\cdot\alpha\text{-}CD\}Fe(CN)_5]^{4-}$	$(0.8 \pm 0.1) \times 10^{-3}$ [e]

[a] $[[(NC)_5Fe(R(CH_2)_npyz)Fe(CN)_5]^{4-}] = 3 \times 10^{-3}$ M, $[Fe(CN)_5D_2O^{3-}] = 1.2 \times 10^{-2}$ M. [b] $[\alpha\text{-CD}] = 4.6 \times 10^{-2}$ M. [c] $[\alpha\text{-CD}] = 3.0 \times 10^{-2}$ M. [d] $[\alpha\text{-CD}] = 6.5 \times 10^{-2}$ M. [e] $[\alpha\text{-CD}] = 4.5 \times 10^{-2}$ M.

of the host can occur. While on steric grounds it might be anticipated that the threading and dethreading of the N-heterocyclic unit through the rim of the α-CD may be easier with the shorter pyrazinium group, the coalescence studies indicate that these processes are considerably slower than for the bipyridinium ligands. It would be expected, based on the relative inclusion stability constants of 4,4′-bipyridine (151 M^{-1}) and pyrazine (20 M^{-1}) ligands with β-CD,[24] that the more hydrophilic pyrazinium head group would form a much weaker inclusion species with α-CD. The threading process therefore involves the removal of solvent from the cationic end units as they enter the α-CD, and resolvation of these groups as they emerge after threading, as well as changes to the interior and exterior solvation of the host α-CD molecule.

The thermodynamic parameters associated with the inclusion equilibria in this study and for the $[bpy(CH_2)_nbpy]^{2+}$ from a previous study are presented in Table 1. The inclusion process is driven by the highly favorable enthalpic effects while being significantly disfavored entropically. It has been proposed that the enthalpies and entropies for the complexation equilibria of a variety of host molecules with a diverse set of guests are not entirely independent of one another, but are in fact compensatory.[27] The change in $T\Delta S$ is proportional to the change in ΔH, leading to eq 22, which upon integration yields eq 23. It was

$$T\Delta(\Delta S) = \alpha\Delta(\Delta H) \quad (22)$$

$$T\Delta S = \alpha\Delta H + T\Delta S_0 \quad (23)$$

concluded that α and $T\Delta S_0$ are quantitative measures of the conformational changes and the extent of desolvation, respectively, upon complex formation. Flexible hosts such as acyclic glymes and cyclic crown ethers undergo substantial conformational change and less extensive desolvation upon binding, affording large slopes (α = 0.76−0.86) and small intercepts ($T\Delta S_0$ = 9.5−10 kJ mol^{-1}).[27a,b] Conversely, the rigid bicyclic cryptands are not able to change their original conformation upon complexation (α = 0.51), but do undergo considerable desolvation ($T\Delta S_0$ = 16.7 kJ mol^{-1}).[27a] From an enthalpy−entropy compensation plot of ΔH against $T\Delta S$ for the α-CD complexes of the ligands in this study and previously reported values for $[bpy(CH_2)_nbpy]^{2+}$ [15] and $[O_2C(CH_2)_nCO_2]^{2-}$ [7] (Figure 5), a slope of α = 0.86 ± 0.10 and an intercept of 12.4 ± 3.2 kJ mol^{-1} are obtained. These parameters are in good agreement with the values determined by Inoue et al. for the inclusion equilibria of α-, β-, and γ-cyclodextrin with a variety of guest molecules; α = 0.90 and $T\Delta S_0$ = 13.0 kJ mol^{-1}.[27c] Employing only the data for α-cyclodextrin a slope of 0.86 is calculated. Molecular mechanics calculations on α-CD inclusion complexes with benzene derivatives indicated that the cavity is distorted, with two opposite glucose units tilted by 40° and the remaining glucose rings by 14°.[28] Inspection of CPK models indicates that the threading of α-CD by the aromatic N-heterocyclic head groups of the $[R(CH_2)_nR]^{2+}$ ligands requires a considerable distortion of the cavity.

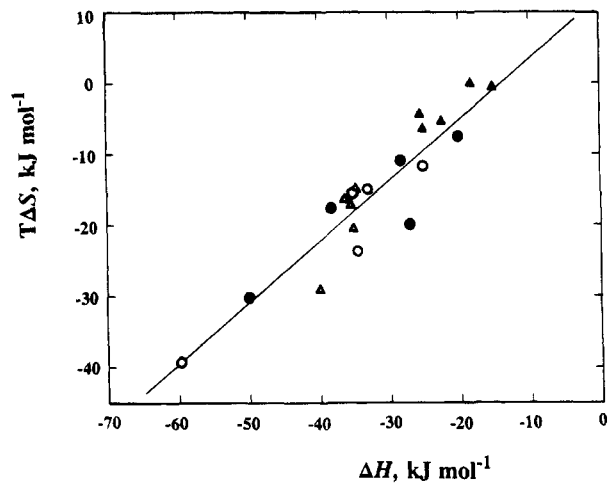

Figure 5. Plot of ΔH against $T\Delta S$ (T = 298 K) for the equilibria involving the α-cyclodextrin inclusion complexes with (●) $[pyz(CH_2)_n pyz]^{2+}$ (this work), (○) $[bpy(CH_2)_npyz]^{2+}$ (this work), (△) $[bpy(CH_2)_n bpy]^{2+}$,[15] and (▲) $[O_2C(CH_2)_nCO_2]^{2-}$[7] guest molecules.

The rate constant for the formation of the substituted monomeric complex, $[Fe(CN)_5(pyz(CH_2)_npyz)]^-$, decreases with an increase in the polymethylene chain length n, with $k_f = 1.13 \times 10^4$ M^{-1} s^{-1} for n = 8 to 0.65×10^3 M^{-1} s^{-1} for n = 11 and 12. This decrease in rate constants with n continues a trend reported previously for this system with n = 3−8, and is due to a reduced stability of the $[Fe(CN)_5OH_2//L]^-$ precursor ion-pair as the charges on the ligand are further separated. The limiting value of approximately 6500 M^{-1} s^{-1} at long chain lengths is roughly twice the rate constants measured for the *N*-methylpyrazinium or $[pyz(CH_2)_{10}Br]^+$ monocations under the same solution conditions (3400 M^{-1} s^{-1}).[26]

The formation rate constants decrease with an increase in added α-cyclodextrin concentrations as a result of a decreased reactivity of included ligands. The limiting rate constants for the reaction of the included ligands (35−55% of the values for the free ligands) are consistent with the entering $\{L\cdot\alpha\text{-}CD\}^{2+}$ ligand appearing to the iron complex to behave as a monocationic species. Inclusion of the polymethylene chain of the ligand in the cavity of α-CD would result in a species in which the two charges on pyrazinium groups would be effecively shielded from each other. The inclusion stability constants determined from these kinetic studies are in good agreement with values obtained from the ^1H NMR chemical shift titrations.

A difference in the rate constants was also observed for the reactions of the $[Fe(CN)_5OH_2]^{3-}$ ion with $[Fe(CN)_5L]^-$ (2000 ± 200 M^{-1} s^{-1}) and $[Fe(CN)_5\{L\cdot\alpha\text{-}CD\}]^-$ (1580 ± 100 M^{-1}

(27) (a) Inoue, Y.; Hakushi, T. *J. Chem. Soc., Perkin Trans. 2* **1985**, 935. (b) Inoue, Y.; Amano, F.; Okada, N.; Inada, H.; Ouchi, M.; Tai, A.; Hakushi, T.; Liu, Y.; Tong, L.-H. *J. Chem. Soc., Perkin Trans. 2* **1990**, 1239. (c) Inoue, Y.; Hakushi, T.; Liu, Y.; Tong, L.-H.; Shen, B.-J.; Jin, D.-S. *J. Am. Chem. Soc.* **1993**, *115*, 475. (d) Inoue, Y.; Liu, Y.; Tong, L.-H.; Shen, B.-J.; Jin, D.-S. *J. Am. Chem. Soc.* **1993**, *115*, 10637.

(28) Schneider, H.-J.; Blatter, T.; Cuber, U.; Juneja, R.; Schiestel, T.; Schneider, U.; Theis, I.; Zimmermann, P. in *Frontiers in Supramolecular Organic Chemistry and Photochemistry*; Schneider, H.-J., Durr, H., Eds.; VCH: Weinheim, 1991; pp 29−56.

Scheme 1

$$[(NC)_5Fe(pyz(CH_2)_nR)Fe(CN)_5]^{4-} \rightleftharpoons [(NC)_5Fe(pyz(CH_2)_nR)]^- + [Fe(CN)_5OH_2]^{3-}$$

$$[(NC)_5Fe(pyz(CH_2)_nR)]^- + \alpha\text{-CD} \rightleftharpoons [(NC)_5Fe\{pyz(CH_2)_nR\bullet\alpha\text{-CD}\}]^-$$

$$[(NC)_5Fe\{pyz(CH_2)_nR\bullet\alpha\text{-CD}\}]^- + [Fe(CN)_5OH_2]^{3-} \longrightarrow [(NC)_5Fe\{pyz(CH_2)_nR\bullet\alpha\text{-CD}\}Fe(CN)_5]^{4-}$$

s^{-1}), where $L^{2+} = [pyz(CH_2)_{10}pyz]^{2+}$. In this instance, the α-cyclodextrin is shielding the incoming $[Fe(CN)_5OH_2]^{3-}$ ion from both the attractive forces of the noncoordinated pyrazinium group and the respulsion from the coordinated $[Fe(CN)_5]^{3-}$ center. The limiting rate constant in this reaction is about half of the limiting value observed in reaction with $[pyz(CH_2)_{10}pyz]^{2+}$ itself, as might be expected statistically. The extent of the decrease in the substitution rate constants upon α-cyclodextrin inclusions of the ligands in both reactions (eqs 8 and 12) is smaller than observed in the case of smaller neutral N-heterocyclic ligands (substituted pyridines and bipyridines).[24] This may be attributed to both a deeper inclusion of N-donor atom and a lack of an electrostatic attraction in the cases of the neutral ligands.

The kinetics of the dissociation of the ligand $[R(CH_2)_npyz]^{2+}$ from the monomeric $[Fe(CN)_5(R(CH_2)_npyz)]^-$ and dimeric $[(NC)_5Fe(R(CH_2)_npyz)Fe(CN)_5]^{4-}$ species were investigated in the absence and presence of α-cyclodextrin. The rate constants for the dissociation reactions of $[Fe(CN)_5L]^-$ were observed to decrease with an increase in the α-CD concentration, as a result of the α-CD inclusion of the coordinated ligand. For $[pyz(CH_2)_npyz]^{2+}$, the extent of the diminution of the rate constant decreases with the length of the polymethylene chain, with decreases of 56% ($n = 8$), 50% (9), 44% (10), 35% (11), and 24% (12) from the non-included ligand rate constants (Table 3). Similar percentage decreases were observed for the two ligand dissociation processes (eqs 17 and 18) involving the $[pyz(CH_2)_nbpy]^{2+}$ ligand. Decreases in the ligand dissociation rate constants have been observed previously in our laboratory upon the α- and β-CD inclusions of coordinated neutral[24] and cationic[23] ligands, and have been attributed in part to a stabilization of the ground state through greater π-back-bonding from the metal to the CD-included N-heterocycle. This explanation is consistent with the observed decrease in this effect as the pyrazinium group is placed further from α-CD cavity with an increasing polymethylene chain length.

The addition of an excess of α-cyclodextrin to solutions of the dimer complexes $[(NC)_5Fe(R(CH_2)_npyz)Fe(CN)_5]^{4-}$ resulted in a slow formation of the corresponding [2]-rotaxane as indicated in Figure 4 for the complex containing the $[pyz(CH_2)_9bpy]^{2+}$ bridging ligand. The rate constants for this process (Table 5) are very similar in magnitude to the values determined for the ligand dissociation reactions of the monomeric and dimeric iron complexes (Table 4). These observations are consistent with our previous study of the complexes containing $[bpy(CH_2)_nbpy]^{2+}$ ligands,[15] and support a mechanism in which the rate-determining step in the rotaxane self-assembly is dissociation of a $[Fe(CN)_5]^{3-}$ unit from the more labile head group of the bridging ligand (Scheme 1). Owing to the greater lability of the 4,4′-bipyridinium group compared with the pyrazinium group, the formation of the rotaxane from the asymmetric dimer should primarily involve a rate-determining dissociation of the Fe−N(bpy) bond.

The $[pyz(CH_2)_nbpy]^{2+}$ ligands may be extended through the reactions of $[pyz(CH_2)_nI]^+$ units with the free nitrogen of the 4,4′-bipyridyl end of the dication yielding a series of $[pyz(CH_2)_nbpy(CH_2)_npyz]^{4+}$ ligands. These bridging ligands afford the preparation of [3]-rotaxanes containing two α-cyclodextrin molecules. We have recently prepared the ligands with $n = 9-11$ and characterized, by ^1H NMR spectroscopy, the rotaxane species $[(NC)_5Fe\{pyz(CH_2)_nbpy(CH_2)_npyz\cdot 2\alpha\text{-CD}\}Fe(CN)_5]^{2-}$ in solution.[29] Further studies on these and related series of pentacyanoferrate(II) [3]- and [4]-rotaxanes of α-cyclodextrin are in progress.

Acknowledgment. We thank the Natural Sciences and Engineering Research Council of Canada for financial support in the form of research and equipment grants (D.H.M.) and Queen's University for a Graduate Scholarship (C.A.W.).

(29) Macartney, D. H.; Waddling, C. A. Manuscript in preparation.